Bond Cleavage

# Homolytic $C_\alpha$–$C_\beta$ Bond Cleavage in a Chiral Alkylarene Radical Cation: Effects of Asymmetric Microsolvation**

*Daniele Catone, Anna Giardini Guidoni, Alessandra Paladini, Susanna Piccirillo, Flaminia Rondino, Mauro Satta, Debora Scuderi, and Maurizio Speranza**

*In memory of Fulvio Cacace*

A "microsolvated" ion consists of an ion that interacts electrostatically with a single neutral molecule. It represents the simplest model for ions generated in a dynamic environment, such as the solvent cage in solution. The main difference is that the behavior of a "microsolvated" ion is not perturbed by those environmental factors (solvation, ion pairing, etc.) that normally affect the fate of intimate ion-dipole pairs in the condensed phase. Hence, a detailed study of the dynamics and the reactivity of microsolvated ions may provide valuable information on the intrinsic factors that govern the reaction and how these factors may be influenced by the solvent cage in solution.

Radical ions are open-shell elusive species of paramount importance in many organic reactions and in biological processes. Oxidative bond breaking and forming involve radical ions and are common processes that take place in asymmetric enzyme cavities. Hence, the knowledge of the effects of an asymmetric microenvironment on the behavior of chiral radical ions is crucial for a more exhaustive comprehension of chiral recognition and rate acceleration by enzymes. Its impact extends to another important field: the abiogenic origin of chirality. Indeed, knowledge of the effects of asymmetric microsolvation on the evolution of chiral species in the isolated state may be key to the elucidation of the "chiral-enrichment" mechanism of chirogenesis, that is, the preferential destruction of a specific enantiomer bound to a chiral selector.

Herein we report a first step in this direction: the measurement of the activation energy for the C–C bond cleavage in the side chain of a chiral alkylarene radical cation and its sensitivity to chiral monosolvation. Side chain $C_\alpha$–$C_\beta$ bond fragmentation in the radical cations of aromatic alcohols is a common process in solution[1–3] whose efficiency is enhanced in polar solvents such as water. Hydrogen bonding between the ion and the solvent in the relevant transition structure is thought to be responsible for the rate acceleration.[4] This hypothesis has been corroborated by recent photoionization studies.[5,6] Mass-resolved resonant two-photon ionization spectroscopy (R2PI-TOF) on a supersonically expanded molecular beam represents a highly accurate tool for determining the energetics of radical ions and their microsolvated derivatives. The energetics of solvation at the microscopic level has been obtained by measuring vibronic spectra, bond-dissociation energies, and IPs (ionization potentials) of various molecular systems.[7] The same experimental approach, combined with computational methods, was recently applied to the first quantitative measurement of the activation barrier of the $C_\alpha$-$C_\beta$ bond cleavage in the (*R*)-(+)-1-phenyl-1-propanol radical cation ($[(BZC_2H_5)_R]^+$) (BZ = PhCHOH) and its monohydrated complex ($[(BZC_2H_5)_R{\cdot}H_2O]^+$).[8] The results indicated that the activation energy of the $C_\alpha$-$C_\beta$ bond cleavage in the bare ion is remarkably higher than that in the monohydrated form. This effect was ascribed to the perturbation induced by the solvent molecule on the position of the intersection between the potential energy surfaces of the two lowest-energy electronic states of the radical cation (Figure 1).

Herein we extend the study to chiral solvent molecules, such as (2*R*,3*R*)-(−)-butanediol ($BD_{RR}$) and (2*S*,3*S*)-(+)-2,3-butanediol ($BD_{SS}$) with the aim of measuring the influence of the *asymmetric microenvironment* represented by the chiral solvent molecule on the efficiency of the $C_\alpha$–$C_\beta$ bond

[*] Dr. D. Scuderi, Prof. M. Speranza
Facoltà di Farmacia, Dipartimento No. 64 (SCTSBA)
Università degli Studi di Roma "La Sapienza"
P.le A. Moro 5, 00185, Roma (Italy)
Fax: (+39) 064-991-3602
E-mail: maurizio.speranza@uniroma1.it
Dr. D. Catone, Prof. A. G. Guidoni, Dr. A. Paladini, Dr. F. Rondino
Dipartimento di Chimica
Università degli Studi di Roma "La Sapienza"
P.le A. Moro 5, 00185 Roma (Italy)
Prof. S. Piccirillo
Dipartimento di Scienze e Tecnologie Chimiche, Università degli Studi di Roma "Tor Vergata"
Via della Ricerca Scientifica, 00133 Roma (Italy)
Dr. M. Satta
IMIP-CNR (Sezione PZ)
85100 Tito Scalo (PZ) (Italy)

[**] This work was supported by the Ministero della Università e della Ricerca Scientifica e Tecnologica (MURST) and the Consiglio Nazionale delle Ricerche (CNR).

  DOI: 10.1002/ange.200353462 

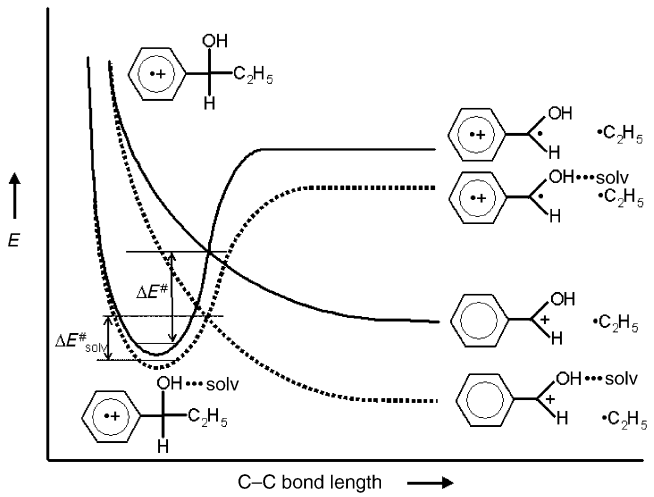


***Figure 1.*** Pictorial crossing between the two lowest-energy electronic states of $[(BZC_2H_5)_R]^+$ (full lines) and $[(BZC_2H_5)_R{\cdot}solv]^+$ (broken lines).

cleavage in $[(BZC_2H_5)_R]^+$. The ionization and fragmentation thresholds of $(BZC_2H_5)_R$ and its clusters with $BD_{RR}$ ($[(BZC_2H_5)_R{\cdot}BD_{RR}]$) and $BD_{SS}$ ($[(BZC_2H_5)_R{\cdot}BD_{SS}]$) were inferred from the onset of the relevant photoionization- and photofragmentation-efficiency curves, respectively, by using a two-color R2PI (2cR2PI) sequence: 1) the first exciting laser ($h\nu_1$) is tuned to the $S_1{\leftarrow}S_0$ transition of the species of interest; 2) the laser intensity is lowered to about 1% of the initial laser-power density to minimize the multiphoton $h\nu_1$ absorption; 3) a second laser ($h\nu_2$) is scanned through the cluster ionization and fragmentation threshold regions of the studied molecular species.

Figure 2a shows the 1cR2PI ($h\nu_1 = h\nu_2$) absorption spectrum of $(BZC_2H_5)_R$ ($m/e = 136$).The three most intense bands were assigned to the three stable conformers of $(BZC_2H_5)_R$ originating from the rotation of the ethyl group around the $C_\alpha{-}C_\beta$ bond.[9] The $S_1{\leftarrow}S_0$ electronic origin of the most stable *anti* conformer and of the two *gauche* rotamers were identified at 37618 (peak B), 37577 (peak A), and 37624 $cm^{-1}$ (peak C), respectively. Figures 1b and 1c show the 1cR2PI absorption spectrum of the heterochiral $[(BZC_2H_5)_R{\cdot}BD_{SS}]$ and the homochiral cluster $[(BZC_2H_5)_R{\cdot}BD_{RR}]$, respectively. The origin of the relevant $\pi{\rightarrow}\pi^*$ electronic transition falls at 37581 $cm^{-1}$ (band $\omega$ of Figure 1b) and 37561 $cm^{-1}$ (band $\theta$ of Figure 1c), respectively. When the same species were submitted to 2cR2PI experiments, the low-energy ($h\nu_2 < 5.5$ eV) ionization ([Eq. (1)] and [Eq. (2)]) and dissociation pathways ([Eq. (3)] and [Eq. (4)]) were observed.

$$\text{Ionization}: \quad [(BZC_2H_5)_R]^* + h\nu_2 \rightarrow [(BZC_2H_5)_R]^+ + e \tag{1}$$

$$[(BZC_2H_5)_R{\cdot}solv]^* + h\nu \rightarrow [(BZC_2H_5)_R{\cdot}solv]^+ + e \tag{2}$$

$$\text{Dissociation}: \quad [(BZC_2H_5)_R]^* + h\nu_2 \rightarrow [BZ]^+ + {}^{\cdot}C_2H_5 + e \tag{3}$$

$$[(BZC_2H_5)_R{\cdot}solv]^* + h\nu_2 \rightarrow [BZ{\cdot}solv]^+ + {}^{\cdot}C_2H_5 + e \tag{4}$$

In these experiments, a particular isomer of a molecular species can be selectively excited by fixing the $h\nu_1$ photon

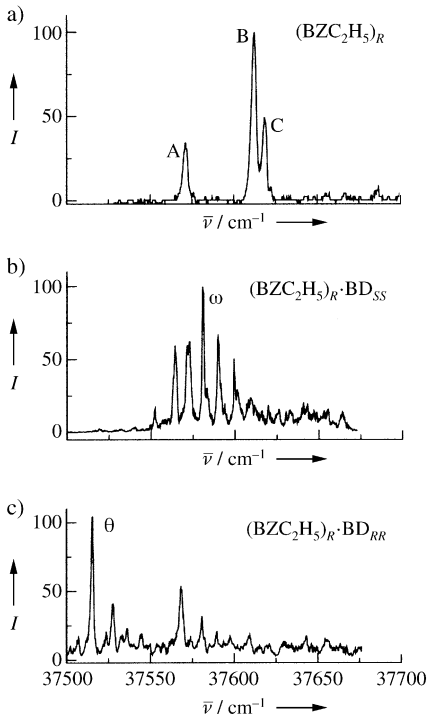


***Figure 2.*** 1cR2PI mass-resolved absorption spectra: a) $(BZC_2H_5)_R$ at $m/e = 136$; b) its heterochiral $[(BZC_2H_5)_R{\cdot}BD_{SS}]$ cluster, and c) its homochiral $[(BZC_2H_5)_R{\cdot}BD_{RR}]$ cluster at $m/e = 226$. BZ = PhCHOH, BD = 2,3-butanediol.

energy at the wavelength of its $S_1{\leftarrow}S_0$ electronic transition and by varying the $h\nu_2$ energy of the second photon. The ionization and fragmentation thresholds of $(BZC_2H_5)_R$ (peak B of Figure 2a; $\nu_1 = 37618\ cm^{-1}$) are reported in Figure 3a.

The onset of the photoionization curve provides a measure of the phenomenological IP of $(BZC_2H_5)_R$ (8.820 ± 0.002 eV). A further increase in the $h\nu_2$ energy leads to the $C_\alpha{-}C_\beta$ bond fragmentation of $[(BZC_2H_5)_R]^*$ with formation of the $[BZ]^+$ ion [Eq. (3)]. The onset of the photofragmentation curve falls at 78610 ± 20 $cm^{-1}$ and provides a value for the ethyl-loss barrier of 7470 ± 40 $cm^{-1}$ above the phenomenological IP of $(BZC_2H_5)_R$. The fragmentation thresholds of Figure 3b were obtained by fixing $\nu_1$ at 37581 $cm^{-1}$ (peak $\omega$ of Figure 2b attributed to the most stable isomer of $[(BZC_2H_5)_R{\cdot}BD_{SS}]$). The ethyl-loss barrier for $[(BZC_2H_5)_R{\cdot}BD_{SS}]^+$ cation was estimated as falling 740 ± 40 $cm^{-1}$ above the phenomenological IP of $[(BZC_2H_5)_R{\cdot}BD_{SS}]$ (70930 ± 20 $cm^{-1}$). In the same way, the fragmentation thresholds of Figure 3c were obtained by fixing $\nu_1$ at 37561 $cm^{-1}$ (peak $\theta$ of Figure 2c attributed to the most stable isomer of $[(BZC_2H_5)_R{\cdot}BD_{RR}]$). The ethyl-loss barrier for $[(BZC_2H_5)_R{\cdot}BD_{RR}]^+$ cation was estimated as falling 1140 ± 40 $cm^{-1}$ above the phenomenological IP of $[(BZC_2H_5)_R{\cdot}BD_{RR}]$ (70580 ± 20 $cm^{-1}$).

The $C_\alpha{-}C_\beta$ bond fragmentation energies ($\Delta E^+$) of $(BZC_2H_5)_R$ and of its homochiral $[(BZC_2H_5)_R{\cdot}BD_{RR}]$ and heterochiral $[(BZC_2H_5)_R{\cdot}BD_{SS}]$ clusters are compared in Table 1 with those previously measured for $[(BZC_2H_5)_R{\cdot}H_2O]$. The marked effect of monosolvation on

  

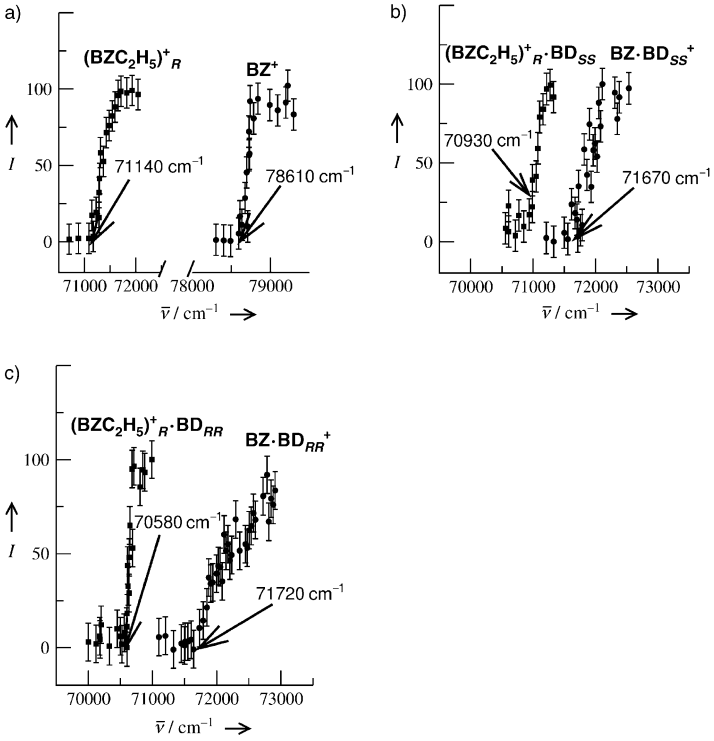


***Figure 3.*** a) 2cR2PI appearance thresholds of the $[(BZC_2H_5)_R]^+$ ion and its ethyl-loss fragment as a function of the total absorbed energy. The excitation photon $\nu_1$ is fixed at 37618 cm$^{-1}$ (see peak B of Figure 2a); b) 2cR2PI appearance thresholds of the $[(BZC_2H_5)_R{\cdot}BD_{SS}]^+$ ion and its ethyl-loss fragment as a function of the total absorbed energy. The excitation photon $\nu_1$ is fixed at 37581 cm$^{-1}$ (see band $\omega$ of Figure 2b); c) 2cR2PI appearance thresholds of the $[(BZC_2H_5)_R{\cdot}BD_{RR}]^+$ ion and its ethyl-loss fragment as a function of the total absorbed energy. The excitation photon $\nu_1$ is fixed at 37561 cm$^{-1}$ (see band $\theta$ of Figure 2c).

***Table 1:*** Ethyl-loss fragmentation energies $\Delta E^{\neq}$ for the unsolvated $[(BZC_2H_5)_R]^+$ and monosolvated $[(BZC_2H_5)_R{\cdot}solv]^+$ ions, and the IPs of the corresponding neutral systems.

| | $\Delta E^{\neq}$ [cm$^{-1}$] | IP [eV] |
|---|---|---|
| $[(BZC_2H_5)_R]$ | 7470 ± 40 | 8.820 ± 0.002 |
| $[(BZC_2H_5)_R{\cdot}H_2O]$ | 3390 ± 40 | 8.709 ± 0.002 |
| $[(BZC_2H_5)_R{\cdot}BD_{RR}]$ | 1140 ± 40 | 8.740 ± 0.002 |
| $[(BZC_2H_5)_R{\cdot}BD_{SS}]$ | 740 ± 40 | 8.776 ± 0.002 |

$\Delta E^{\neq}$ is evident. It essentially reflects the strong stabilization of the incipient closed-shell $[BZ]^+$ ion caused by the solvent molecule. As shown in Figure 1, the intersection between the PES (potential energy surface), adiabatically correlated with the ionic open-shell biradical $\cdot[BZ]^{+\cdot}$ ion, and the PES, adiabatically correlated with the closed shell $[BZ]^+$ ion, generates the energy barrier for the ethyl radical loss in $[(BZC_2H_5)_R]^+$. In the $[(BZC_2H_5)_R]^+$ fragmentation, the unpaired $C_\alpha$ electron, which arises from the homolytic $C_\alpha$–$C_\beta$ bond cleavage, is transferred to the ring of $\cdot[BZ]^{+\cdot}$ to pair its singly occupied $\pi_{SOMO}$ orbital. As a consequence, the positive charge, initially dispersed over the entire $\cdot[BZ]^{+\cdot}$ structure, is essentially localized on the $^+C_\alpha$–OH⇄$C_\alpha$=$OH^+$ group of the closed-shell $[BZ]^+$ ion. The solvent dipole interacts more favorably with the $^+C_\alpha$–OH⇄$C_\alpha$=$OH^+$ group of $[BZ]^+$ than with the $C_\alpha$–OH group of $[(BZC_2H_5)_R]^+$ as most of the positive charge in this latter ion is dispersed over the aromatic ring.

Along these lines, the more basic the solvent molecule, the more pronounced is the $C_\alpha$=O···$H^+$···solv proton transfer and the larger is the stabilization of the $[(BZ{\cdot}solv]^+$ fragment. Therefore, the activation barrier of the homolytic $C_\alpha$–$C_\beta$ bond cleavage in $[(BZC_2H_5)_R{\cdot}solv]^*$ should decrease appreciably from solv = $H_2O$ (proton affinity = 165 kcal mol$^{-1}$)[10] to solv = 2,3-butanediol (proton affinity = 206 kcal mol$^{-1}$),[11] as actually observed (Table 1). However, closer inspection of Table 1 reveals that the activation barrier of the homolytic $C_\alpha$–$C_\beta$ bond cleavage in the heterochiral $[(BZC_2H_5)_R{\cdot}BD_{SS}]^+$ complex ($\Delta E^{\neq} = 740 \pm 40$ cm$^{-1}$) is significantly lower than that in the homochiral $[(BZC_2H_5)_R{\cdot}BD_{RR}]^+$ complex ($\Delta E^{\neq} = 1140 \pm 40$ cm$^{-1}$), in spite of the identical basicity of the *isolated* diol enantiomers.

This difference must therefore be related to the opposite configuration of the diol molecule in the diastereomeric $[(BZC_2H_5)_R{\cdot}BD_{SS}]^+$ and $[(BZC_2H_5)_R{\cdot}BD_{RR}]^+$ complexes. It is well established that cooperative intramolecular O–H···O–H interactions are present in these systems,[12] whose geometric features depend on the specific configuration of the diol moiety (Figure 4). In particular, the heterochiral complex

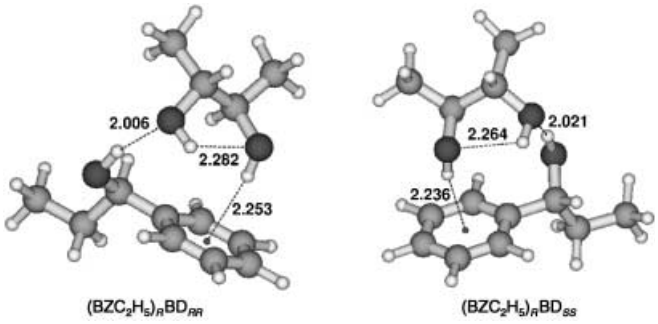


***Figure 4.*** $[(BZC_2H_5)_R{\cdot}BD_{SS}]$ and $[(BZC_2H_5)_R{\cdot}BD_{RR}]$ cluster equilibrium geometries predicted by molecular-dynamics conformational minima search.[12]

exhibits shorter O–H···O–H and O–H···π hydrogen-bond distances than the homochiral adduct. This implies that $BD_{SS}$ is a better H-bond acceptor than $BD_{RR}$ when associated with the chiral $(BZC_2H_5)_R$ moiety. The measured difference in the activation barrier of the homolytic $C_\alpha$–$C_\beta$ bond cleavage in the diastereomeric $[(BZC_2H_5)_R{\cdot}BD_{SS}]^+$ and $[(BZC_2H_5)_R{\cdot}BD_{RR}]^+$ complexes can be rationalized if they are formed with the same structure of their neutral precursors, that is, by a vertical electronic transition.

In conclusion, the activation barriers of the homolytic $C_\alpha$–$C_\beta$ bond cleavage in $(BZC_2H_5)_R$ and its homochiral $[(BZC_2H_5)_R{\cdot}BD_{RR}]$ and heterochiral $[(BZC_2H_5)_R{\cdot}BD_{SS}]$ clusters are much lower than the typical C–C bond energies (80–90 kcal mol$^{-1}$). Their magnitude decreases when the chromophore is bound to solv = water or 2,3-butanediol. The barrier is influenced by the hydrogen-bonding interaction between solv and the OH group of $(BZC_2H_5)_R$ in $[(BZC_2H_5)_R{\cdot}solv]^+$,

  

which affects the charge-transfer process from the ring to the $C_\alpha$ of the incipient $[BZ]^+$ moiety. The different basicities of water and 2,3-butanediol is reflected in the larger $C_\alpha$–$C_\beta$ bond-cleavage activation barrier for $[(BZC_2H_5)_R{\cdot}H_2O]^+$ than those for the ionic clusters with diols as solv. The activation barrier of the $C_\alpha$–$C_\beta$ bond cleavage for the heterochiral $[(BZC_2H_5)_R{\cdot}BD_{SS}]^+$ cluster is about two thirds that for the homochiral $[(BZC_2H_5)_R{\cdot}BD_{RR}]^+$. This difference may be attributed to structural factors that make solv in the former adduct a better H-bond acceptor than in the latter, although other hypotheses, such as that involving the interaction of the solvent molecule with the $C_\alpha$ center of $[(BZC_2H_5)_R]^+$ cannot be excluded.

## Experimental Section

The experimental setup combines a supersonic molecular beam with a homebuilt TOF spectrometer. The supersonic expansion is produced by a General valve pulsed nozzle ($T = 120\,°C$, opening time 200 μs, internal diameter 400 μm). The carrier gas (Ar, stagnation pressure: 2–4 atm) is mixed with $(BZC_2H_5)_R$ and $BD_{RR}$ or $BD_{SS}$ ($T = 120\,°C$). The relevant 1:1 clusters are formed in the adiabatic supersonic expansion. The concentration of the seeding molecules is maintained low enough to minimize the production of larger clusters. The skimmed supersonic jet (1 mm skimmer diameter) enters a second chamber equipped with the TOF mass spectrometer. Molecules and clusters are excited and ionized by one or two tunable dye laser beams. The detection of the ionized species is performed through a channeltron. The signals, recorded and averaged by a digital oscilloscope, are stored and processed on a PC.

Received: December 5, 2003 [Z53462]

**Keywords:** asymmetric microsolvation · cluster compounds · enantioselectivity · photoelectron spectroscopy · radical reactions

[1] E. Baciocchi, O. Lanzalunga, M. Bietti, *Acc. Chem. Res.* **2000**, *33*, 243.
[2] P. Mislak, *Top. Curr. Chem.* **1993**, *168*, 1.
[3] R. Popielarz, D. R. Arnold, *J. Am. Chem. Soc.* **1990**, *112*, 3068.
[4] E. Baciocchi, M. Bietti, L. Putignani, S. Steenken, *J. Am. Chem. Soc.* **1996**, *118*, 5952.
[5] J. Yao, H. S. Im, M. Foltin, E. R. Bernstein, *J. Phys. Chem. A* **2000**, *104*, 6197.
[6] R. Weinkauf, L. Lehr, A. Metsala, *J. Phys. Chem. A* **2003**, *107*, 2727.
[7] S. Piccirillo, C. Bosman, D. Toja, A. Giardini Guidoni, M. Pierini, A. Troiani, M. Speranza, *Angew. Chem.*, **1997**, *109*, 1816; *Angew. Chem. Int. Ed. Engl.* **1997**, *36*, 1729.
[8] S. Piccirillo, M. Satta, D. Catone, D. Scuderi, A. Paladini, F. Rondino, M. Speranza, A. Giardini Guidoni, unpublished results.
[9] A. Latini, M. Satta, A. Giardini Guidoni, S. Piccirillo, M. Speranza, *Chem. Eur. J.* **2000**, *6*, 6.
[10] S. G. Lias, E. P. L. Hunter, *J. Phys. Chem. Ref. Data* **1998**, *27*, 413.
[11] Estimated from the PA limits of secondary alcohols (J. Long, B. Munson, *J. Am. Chem. Soc.* **1977**, *99*, 6822) by using the group additivity method (S. W. Benson, *Thermochemical Kinetics*, Wiley, New York, **1968**).
[12] D. Scuderi, A. Paladini, M. Satta, D. Catone, F. Rondino, M. Tacconi, A. Filippi, S. Piccirillo, A. Giardini Guidoni, M. Speranza, *Phys. Chem. Chem. Phys.* **2003**, *5*, 4570.

  